

Sediment dynamics of a sandy contourite: the sedimentary context of the Darwin cold-water coral mounds, Northern Rockall Trough

V. A. I. Huvenne · D. G. Masson · A. J. Wheeler

Received: 29 January 2007 / Accepted: 11 March 2008 / Published online: 4 April 2008
© Springer-Verlag 2008

Abstract Grainsize, mineralogy and current-meter data from the Northern Rockall Trough are presented in order to characterise the sandy contourite that forms the sedimentary environment of the Darwin cold-water coral mounds, and to investigate the impact of this environment on the mound build-up. Large clusters of small cold-water coral mounds, 75 m across and 5 m high, have been found southwest of the Wyville Thomson Ridge, at 900–1,100 m water depth. Their present-day sedimentary environment consists of a subtly sorted sandy contourite, elongated NE–SW, roughly parallel to the contours. Critical erosional and depositional current speeds were calculated, and trends in both the quartz/feldspar and foraminifera fractions of the sands show a bi-directional fining from bedload/erosion-dominated sands in the NE to suspension/deposition-dominated sediments in the SW and towards the S (downslope). This is caused by a gradual reduction in governing current speed, linked to a reduction in slope gradient, and by the increasing distance from the current core in the downslope direction. No specific characteristics were found distinguishing the mound sediments from the surrounding sands: they fit in the overall spatial pattern. Some mound cores show hints of a fining-upward trend. Overall the mound build-up process is interpreted as a result of sediment baffling.

Keywords Cold-water corals · Sandy contourites · Sediment transport · Continental margin · Northern Rockall Trough

Introduction

The seabed in Northern Rockall Trough shows a variety of bottom current induced sedimentary features, such as different types of sediment drifts and thin sandy contourite sheets (Howe et al. 2002; Laberg et al. 2005). Within this environment, on the upstream flank of a broad sheeted drift, the Darwin mounds were discovered in 1998 during a TOBI sidescan sonar survey (Towed Ocean Bottom Instrument; Masson and Jacobs 1998). Further investigations (Bett et al. 2001) revealed that the small mounds, up to 75 m across, are colonised by cold-water corals (*Lophelia pertusa* L.) and associated fauna, and mainly contain sandy sediments. The surrounding seafloor is covered by a relatively thin, rippled, contourite sand sheet, overlying thick sequences of glaciomarine mud (Masson et al. 2003).

The origin of cold-water coral reefs, banks or mounds has often been a cause for debate. The corals themselves, also referred to as deep-water corals, are known to require a hard substrate for settlement (although this could be a shell or dropstone), sufficient nutrient input, a certain temperature and salinity range (ca. 4–12°C and 34–37‰) and an enhanced current regime that helps them keep free from sediments and increases the nutrient flux (Freiwald 2002). However, the initiation of reef growth has been attributed by, for example, Hovland (1990) and Henriot et al. (1998) to fluid (i.e. methane) seepage locally fertilising the water column, resulting in increased concentrations of bacteria and other micro-organisms and creating a hard substrate through authigenic carbonate formation. Amongst others,

V. A. I. Huvenne (✉) · D. G. Masson
National Oceanography Centre, Southampton,
European Way, Southampton SO14 3ZH, UK
e-mail: vaih@noc.soton.ac.uk

A. J. Wheeler
University College Cork, Cork, Ireland

De Mol et al. (2002) and Freiwald et al. (2002) on the other hand suggest that the mound and reef development is related to benthic–pelagic coupling and the occurrence of the correct oceanographic conditions. Mienis et al. (2007) for example present data from coral reef areas in the SE and SW Rockall Trough which illustrate very well the presence of tidal influences, particle fluxes and nepheloid layers. Initial coral colonies forming patches on the seabed would be able to baffle sediments, which would gradually result in mound formation (see also the review by Roberts et al. (2006)).

In the specific case of the Darwin mounds, Masson et al. (2003) suggested that, based on comparability in size and shape, both the mounds and a set of pockmarks on the down-current side of the sediment drift are caused by fluid expulsion, most probably of pore waters. Mounds occurred in areas where the fluid escape brought up sandy materials, too heavy for the bottom currents to disperse. The pockmarks were formed in finer sediments, which could be washed away by currents when destabilised by seepage. The hypothesis therefore suggested that the cold-water corals colonised the mounds (because they provided an elevated substrate) rather than mounds being formed through trapping of sediments in the coral frameworks.

Despite the lasting uncertainties concerning cold-water coral mound origin, intensive research over the last decade or so (see for example Freiwald and Roberts 2005) brought a general consensus that the local hydrodynamic regime and the sedimentary environment play a major role in mound development (e.g. Kenyon et al. 2003; Mienis et al. 2006; Huvenne et al. 2007). In the case of the Darwin mounds, this environment is represented by the sandy contourite, a type of deep-sea sedimentary system that is still not fully understood in its own right, even if contourite research has an economic importance and gradually attracts more interest (Viana et al. 2007).

The work presented in this paper, based on the study of a set of piston and boxcores of the Darwin mound area, therefore has two objectives: (1) to present the sedimentary environment of the Darwin mounds, i.e. the sandy contourite, mainly from a hydrodynamic/sediment dynamic point of view, in order to gain insight in the formation mechanisms of contourites; and (2) to discuss the impact of this sedimentary environment on the mounds and their build-up, in order to increase the understanding of the formation of small cold-water coral mounds.

Setting

Geology

The Rockall Trough is a south-westerly trending basin, separating the Rockall Bank from Scotland and Ireland.

Water depths range from 1,000 m in the NE to over 4,000 m in the SW, where the Trough opens towards the Porcupine Abyssal Plain (Fig. 1). It is on average 200–250 km wide, and is underlain by a greatly thinned continental crust (Stoker et al. 1993). Towards the NE, the Rockall Trough is bound by the Wyville–Thomson Ridge (WTR), a transverse bathymetric high, nearly perpendicular to the Hebrides shelf edge and rising up to water depths of less than 400 m. It is formed of Paleogene basalts and sediments, and creates a major topographic barrier between the Rockall Trough and the Faroe–Shetland Channel (Roberts et al. 1983). Its steep flanks are covered by Plio- and Pleistocene deposits, and contourite drifts have been found on its lower slopes.

The sediment drift complex at the base of the WTR is described in detail by Howe et al. (1994), Stoker et al. (1998) and Masson et al. (2002). It consists of three sediment drift types: an elongated drift of ca. 60 km long on the eastern margin, with slope-parallel moat and drift crest; a broad sheeted drift on the western margin, on the southeastern flank of the Ymir Ridge, with a crest perpendicular to the slope; and several moat-related subsidiary or patch drifts (Fig. 1). They mainly consist of Miocene, Pliocene-early Pleistocene (Lower MacLeod Fm) and upper Pleistocene-lower Holocene (MacAulay Fm) sequences. The sheeted and elongated drifts are partially covered by the sediments and debris flows of the Sula Sgeir fan and slope apron, which was predominantly active during the Pleistocene glaciations (Howe et al. 1994). Both relict and active sediment waves have been found at several locations on the larger drift bodies (Masson et al. 2002).

In terms of the current seabed sediments in the Northern Rockall Trough, large areas on the upper slopes of the WTR and the Hebrides margin are covered by gravels, in many places cut by iceberg ploughmarks (Belderson et al. 1973; Stoker et al. 1993). On the lower slopes (ca. 900–1,200 m), a wide range of cores illustrate that the general sedimentary sequence consists of hemipelagic and/or glaciomarine muds, overlain by thin sandy contourite sheets, indicative of an increase in current velocity related to the Holocene deglaciation (Howe et al. 1994; Masson et al. 2002; Laberg et al. 2005). The terrigenous materials in the contourites are mainly of local origin, reworked from the underlying Pleistocene deposits. However, although the basin has been starved of terrigenous sediment input during the Holocene, the biogenic, carbonate-rich input (e.g. foraminifera) was high.

Hydrography

The WTR forms a major barrier between the Northern Rockall Trough and the Faroe–Shetland Channel, strongly controlling water mass exchange between the two. From a

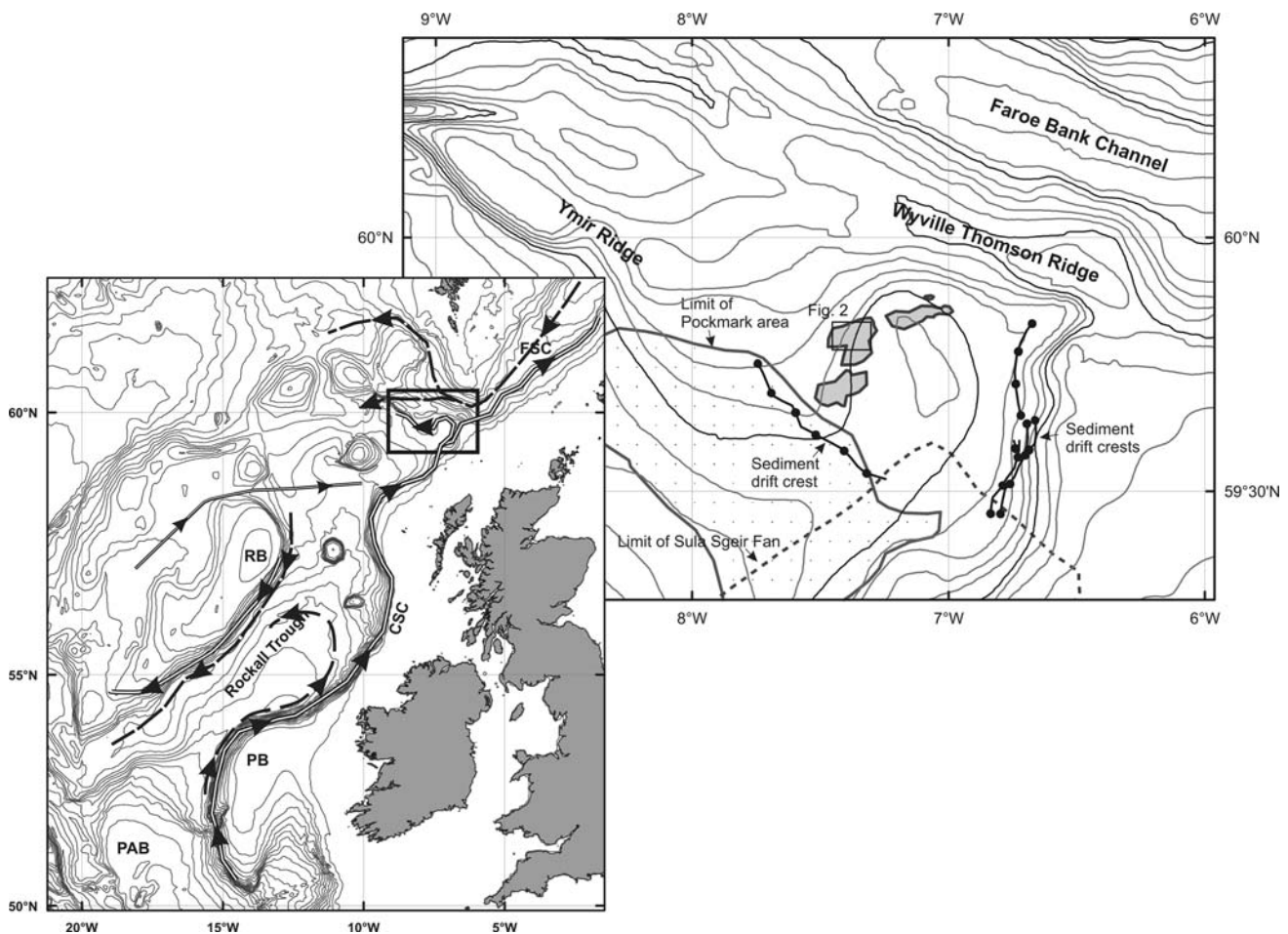


Fig. 1 Overview map of the study area, indicating the main clusters of Darwin mounds as grey shaded polygons. Bathymetric contour interval: 100 m. The locations of the sediment drift crests, pockmark area and limit of Sula Sgeir fan deposits are mapped after Masson et al. (2003) Inset: hydrographical setting of the Rockall Trough, indicating the major surface and deep-water currents affecting the

Darwin mound area with *continuous* and *broken lines* respectively. Bathymetric contour interval: 200 m CSC continental slope current (as defined by Hansen and Østerhus (2000)), FSC Faroe–Shetland Channel, PAB porcupine abyssal plain, PB Porcupine Bank, RB Rockall Bank

wider point of view, this is a key area for the water mass exchange between the Atlantic and Arctic Oceans, and hence for global circulation as a whole. Cold and dense Norwegian Sea Deep Water (NSDW) is funnelled southwards through the Faroe–Shetland and Faroe Bank Channels, and enters the Atlantic, together with a certain amount of Norwegian Sea Arctic Intermediate Water (NSAIW), when it crosses the 840 m deep sill at the NW end of the Faroe Bank Channel (Hansen and Østerhus 2000; and references therein). A limited amount of NSDW and NSAIW also crosses the western WTR and Ymir Ridge, and flows southwards into the Rockall Trough (Ellet and Roberts 1973; Ellet 1998). Once across the overflow, the dense watermasses descend rapidly under the Labrador Sea Water (LSW, present between ca. 1,600 and 1,900 m, Ellet et al. 1986), entraining and partly mixing with it as they sink. Further admixture of deeper Antarctic Bottom

Water results in the formation of the North East Atlantic Deep Water (NEADW) which flows southwards along the western margin of the Rockall Trough (New and Smythe-Wright 2001). The exact circulation patterns of these deeper waters are not always well understood, but several anticlockwise gyres seem to be formed in the deeper parts of the Rockall Trough (2,000–3,000 m, Knutz et al. 2002; Laberg et al. 2005).

The opposite flow from the Rockall Trough into the Faroe–Shetland Channel basically consists of Eastern North Atlantic Water (ENAW, or NEAW according to Howe et al. (1994) and Stoker et al. (1998)), with a limited addition of Modified North Atlantic Water (MNAW) brought into the Rockall Trough and across the WTR by a branch of the North Atlantic Current (Hansen and Østerhus 2000). The ENAW is carried northwards along the eastern slope of the Rockall Trough by the Continental Slope

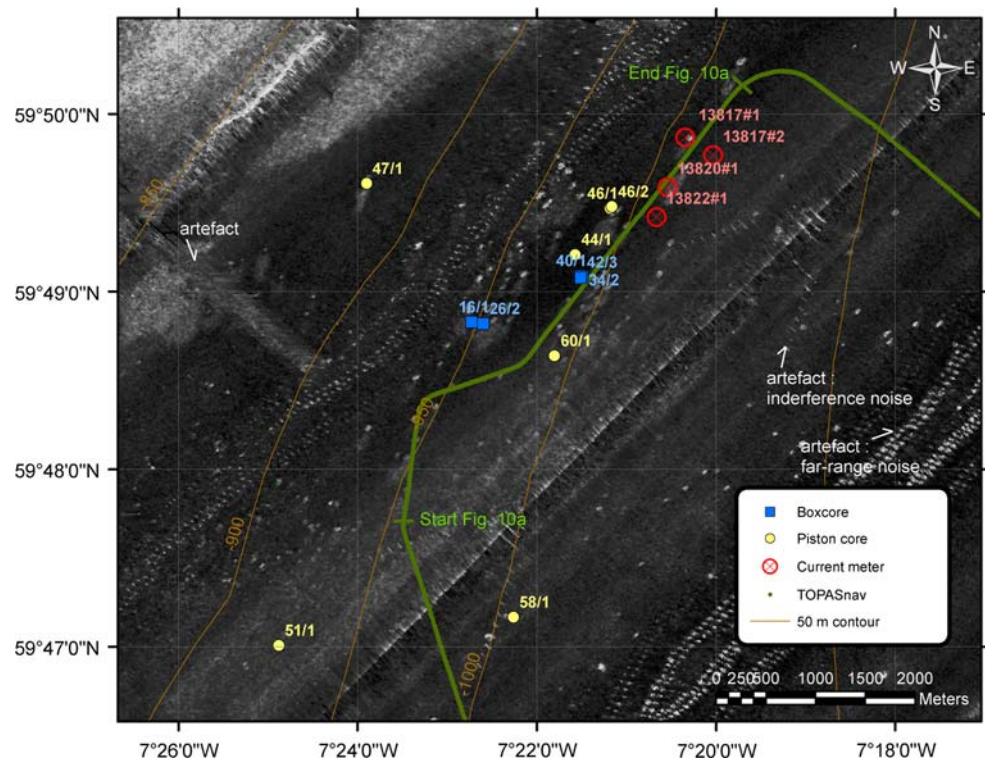
Current (CSC). The flow is strongest at shallow depths, above the 500 m contour (typically less than 200 m (Burrows and Thorpe 1999)), but the ENAW and the northward CSC do reach down to depths of 1,000–1,200 m (Ellet et al. 1986; Stoker et al. 1998). Howe and Humphery (1995) measured peak bottom currents of 15 cm/s at 1,035 m depth on the Hebrides slope, and mention current fluctuations, possibly of tidal origin. When reaching the WTR, the main part of the CSC crosses this barrier, but the deeper part (>500 m) is partly detached, and is deflected northwest- to westward along the WTR and further southward along the eastern flank of the Ymir Ridge (Huthnance 1986; Howe et al. 1994, 2002; Hansen and Østerhus 2000). It is along this deflected path that the broad sheeted drift described by Howe et al. (1994), Stoker et al. (1998) and Masson et al. (2002) could build up. Sedimentary bedforms such as ripples, developed in the sandy contourite sheets, suggest peak currents of >25–30 cm/s (Masson et al. 2002). Indeed, Masson et al. (2003) mention maximum current velocities of ca. 35 cm/s in a south-westerly direction. Again there seems to be evidence for a strong tidal influence (see also “Current meter records”).

The Darwin mounds

In this specific setting of the Northern Rockall Trough, in the embayment between WTR and Ymir Ridge, the Darwin mounds were found in water depths ranging from 900 to

1,100 m. They occur in four major groups, more than 300 mounds in total. On 30 kHz TOBI sidescan sonar imagery they are easily recognised as sub-circular high-backscatter patches contrasting with the low-backscatter background that characterises the well-sorted contourite sands (Fig. 2). They are some 75–80 m across, and on echosounder profiles they are represented by low-amplitude convex reflections, reaching a maximum of 5 m above the surrounding seabed. Towards the south–west the mounds tend to become even lower, until they lose all vertical expression close to the crest of the broad sheeted drift, and are only represented on the profiles by hyperbolae (Masson et al. 2003; Wheeler et al. 2008). Further to the south-west, across the drift crest, a large field of pockmarks of similar size (ca. 50 m diameter) was found (Fig. 1), prompting Masson et al. (2003) to their suggestion that both pockmarks and mounds were formed by some type of fluid expulsion, most probably of pore waters. Other authors (e.g. Hovland et al. 1987; Hovland and Judd 1988) have often related such features to hydrocarbon seepage (e.g. gas). Kiriakoulakis et al. (2004), however, carried out sorbed gas and lipid analyses on piston core sediments (up to 8.2 m deep) in the area. The low concentrations of sorbed methane and of high molecular weight hydrocarbons, together with the typical terrestrial, rather than petrogenic, signature of biomarkers (high molecular weight fatty acids) confirmed that there is no evidence to suggest that the Darwin mounds are affected by any type of hydrocarbon seepage.

Fig. 2 Location map of the cores, current meters and TOPAS profile used. Background: TOBI sidescan sonar imagery, after Masson et al. (2003), showing the high-backscatter mound and tail features (light colours) against the low-backscatter background (dark colours)



Most of the larger mounds are associated with a tail-structure, an elongated patch of moderate backscatter stretching in the direction of the prevailing bottom currents (Fig. 2). These do not have any measurable signature on the 3.5 kHz profiler data, are not apparent on higher frequency (100 and 410 kHz) side-scan sonar (Wheeler et al. 2008), and are gradually less distinct or even absent towards the crest of the sediment drift. They have been interpreted by Masson et al. (2003) as downstream scouring-related or current-related features.

The main cold-water coral species encountered on the Darwin mounds is *Lophelia pertusa* L. (Bett 2001), although Masson et al. (2003) also mention *Madrepora oculata* L. and a variety of other associated species. The corals occur mainly on the tops of the mounds, whereas on the “mounds without relief” (towards the SW) only a limited amount of live coral was found, together with accumulations of coarse sediments and debris. In general, the coral colonies appear rather scattered: Masson et al. (2003) report average coral densities of one colony per 4 m².

Very high resolution sidescan sonar surveys over the Darwin mounds also revealed severe trawling damage in this area (Wheeler et al. 2005b). Several coral colonies and mounds were smashed into pieces, and trawl marks could be seen on the seafloor. As a result of these findings, the European Commission adopted a regulation in March 2004 to permanently ban bottom trawling from the Darwin mound area, while the UK government has the intention to designate the province as special area of conservation (SAC) under the Habitats Directive.

Materials and methods

Sedimentology

The key data source for this study was a set of piston and boxcores, collected during the RRS Discovery cruise 248 in 2000 in the Northern Rockall Trough. From the entire set of cores, also described briefly in Masson et al. (2003), a limited number were selected for detailed study. They represent specific environments such as ‘mounds’, ‘background sediments’, and ‘tails’ (Figs. 2 and 3). The main aim was to try to identify sediment types with different characteristics (especially in the sand fraction), in order to determine differences in the sediment origin and/or deposition history.

The piston cores, with a diameter of 7 cm, were sampled at least every 40 cm, and extra samples were taken to characterise unit boundaries or localised changes in sediment properties. Subcores from the boxcores were sampled in each sedimentary layer. The samples (ca. 4 cm³) were

dried, weighed and wet sieved at 63 µm to separate sand and mud. The sand fraction, when >20%, was further sieved over 13 sieves ranging from 500 µm (1φ) to 63 µm (4φ), with intervals of 0.25φ. The mud fraction was analysed using a Sedigraph 5100, for those samples where the fraction exceeded 20%. Based on the grainsize results, five sand size classes were chosen, of varying interval length, with the narrowest classes around the interval where most samples have their main sand mode (i.e. between 2.25 and 3.25φ, see Table 1). In this way, the most important parts of the grainsize curves could be captured in more detail. In each of the classes, the mineralogical/grain composition of 17 key samples was determined. For each sample and class, at least 300 grains (if available) were identified under the binocular microscope and classified in one of the 14 classes listed in Table 2.

Supporting data sets

In order to place the cores in their spatial context, additional data sets were used to provide supporting background information. These include 30 kHz TOBI sidescan sonar imagery and 3.5 kHz profiles, collected during the same cruise in 1998, and a high resolution topographic parametric sonar (TOPAS) subbottom profile collected in 2003. The sidescan sonar imagery, also published in Masson et al. (2003) was processed with the NOCS PRISM software (LeBas 2002), while the TOPAS profile was processed using the freeware ‘Seismic Unix’ (Cohen and Stockwell 2002). All spatial information was integrated within a geographical information system (GIS), using the ArcGIS software suite, in order to obtain an integrated interpretation.

Furthermore, during the RRS Discovery cruise 248 in 2000, four Aanderaa current meters were deployed at closely-spaced locations on and between the Darwin mounds (Fig. 2). They were positioned at ca. 1 m above the seabed, and recorded temperature, current speed and direction for ca. 20 days.

Results

Grainsize

The results from the grainsize analyses are summarized in Figs. 3 and 4, and the overall pattern in the cores confirms the descriptions by Masson et al. (2003). The mound cores (46/1, 46/2, 58/1 and 60/1) contain sandy sediments throughout, while the off-mound cores (47/1 and 51/1) mainly contain mud, overlain by a thin layer of muddy sand and sand. Also the boxcores, taken in the ‘tails’, fit into this overall pattern: being off-mound cores, they

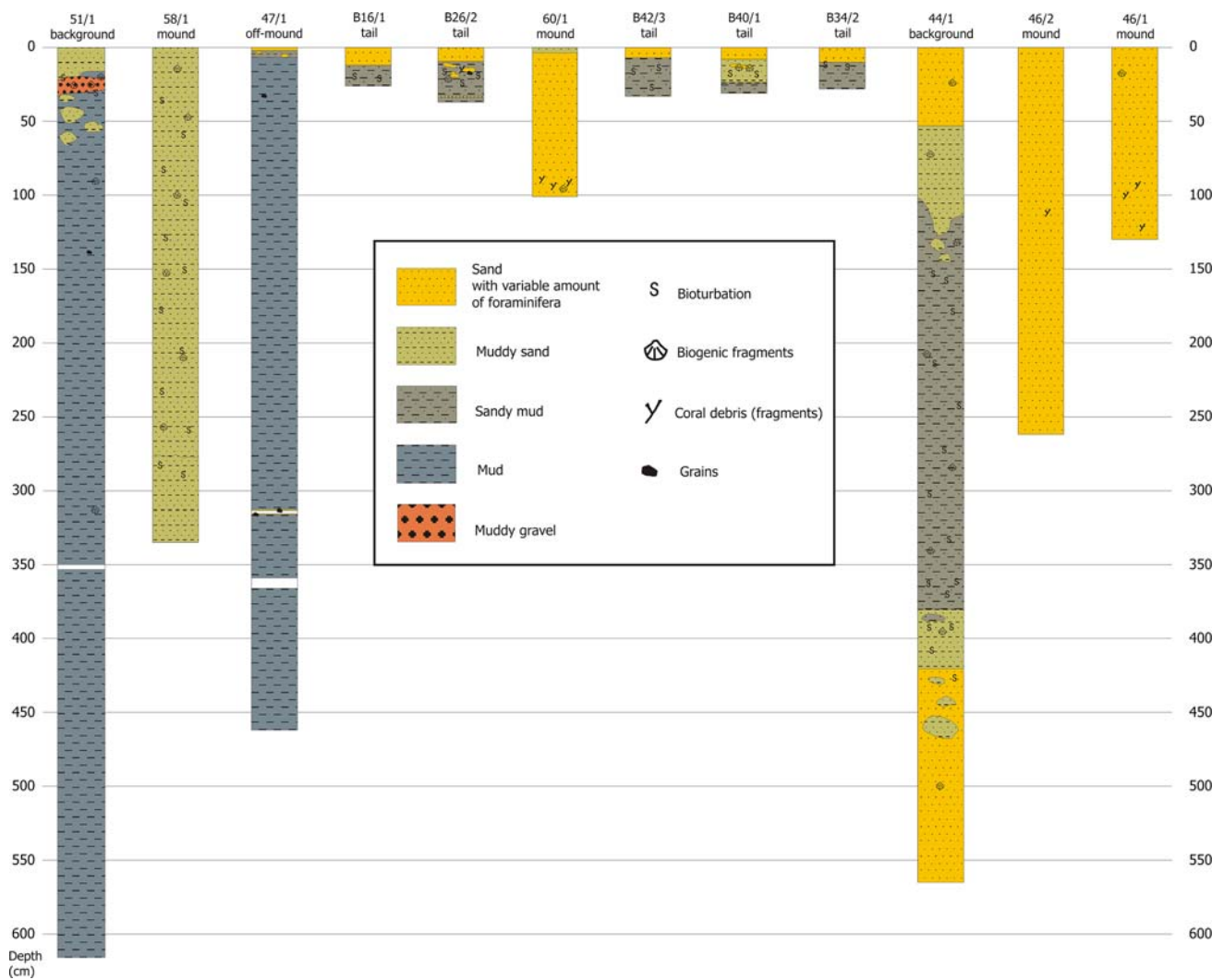


Fig. 3 Core drawings of the cores used in this study

Table 1 Class boundaries of the five sand classes used for the mineralogical analysis

	Lower boundary (ϕ)	Upper boundary (ϕ)	Lower boundary (μm)	Upper boundary (μm)
Class 1	1		500	
Class 2	2.25	1	210	500
Class 3	2.75	2.25	150	210
Class 4	3.25	2.75	106	150
Class 5	4	3.25	63	106

contain the upper sequence of the muddy sands overlain by sand. Only core 44/1 shows an unusual pattern: although it is taken in the ‘background’, it is much sandier than cores 47/1 and 51/1, and includes a fining upwards and coarsening upwards sequence, with an irregular unconformable contact between the upper sandy and underlying muddy

units (Fig. 3). Another intriguing observation is the presence of a large amount of gravel in a reddish muddy matrix in core 51/1, where it marks the contact between the top sand and lower grey mud (Fig. 3).

The grainsize distributions of the sandy sediments show patterns described by Michels (2000) as typical for ‘well-sorted’ or ‘residual’ sediments. These have a narrow range of grain sizes or generally lack the fine fractions (<10% mud) and are typical for areas under the influence of contour currents. The muddy sediments on the other hand show the opposite pattern: they have a broad, uniform distribution without any clear mode. Michels (2000) identifies such sediments as ‘low-energy depositional’. According to McCave and Hall (2006) the lack of sorting in such fine sediments may be due to the effect of flocculation during deposition. Because the dominant mode—reflecting the current influence on the area—generally occurs within the sand grain sizes, and because the mounds

Table 2 Components identified during the mineralogical analysis, with the density values used to convert the grain counts (approximation of volume percentages) to approximate weight percentages

Mineralogical class	Density (kg/m ³)
Quartz/feldspar	2,650
Lithic fragments	2,650
Muscovite	2,800
Biotite	3,000
Glaucinite	2,800
Hornblende	3,000
Flint	2,650
Foraminifera	1,500
Biogenic fragments	2,000
Spicula	2,000
Echinoid spines	2,000
Ostracods	1,500
Unidentified	2,650
Obsidian	2,650

are built up of sandy sediments, the focus of the analyses was placed on this fraction of the sediment samples.

The different sedimentary facies show moderate bioturbation, especially in the muddy sands/sandy muds, resulting in burrowed contacts with over- and underlying facies. Overall, most of the contacts are sharp, except for some in core 44/1 (Figs. 3 and 4). Very few coral fragments were encountered in the mound cores: there is no coral framework supporting the sediments. With their very low mud content, the mound cores are homogeneous. Only in core 60/1, the sands become slightly finer towards the top, where they grade into muddy sands. However, when compared with each other, there seems to be a fining in the mound-core sediments from the N–NE of the study area to the S–SW, and from shallower to deeper waters (from cores 46/1 and 46/2 over 60/1 to 58/1). A similar trend can be observed in the upper sands of the off-mound cores (See Figs. 2 and 4a).

Mineralogy

Overall, the mineralogical composition of the sands is dominated by quartz and feldspar grains (ca. 43–88%) and foraminifera (5–40%), and in lesser amount by unidentified biogenic fragments (1.4–14%), lithic fragments (0.7–2.7%) and glauconite (0.4–3.2%). This is illustrated in Fig. 5, which shows the composition of the five chosen grain size classes for three representative samples. The results of the first class (>500 μm) have to be interpreted with care, because in most cases far less than 300 grains were available, and therefore these results may not be entirely representative.

No minerals/grain types were encountered that were exclusive for either mound or off-mound samples, which suggests a single provenance for the sands. The ratio of the different constituents varies between the different grain size classes, with the foraminifera more dominant amongst the larger grains, quartz and feldspar dominant in classes 4 (106–150 μm) and 5 (63–106 μm), and the unidentified (often broken) biogenic fragments contributing mostly to classes 1 (>500 μm) and 5 (63–106 μm). The ratio of foraminifera versus quartz/feldspar in class 3 (150–210 μm) is variable, and is at least partially related to the overall sand grain size distribution and current sorting effects (smaller mean grain size = lower quartz/feldspar content in class 3 (150–210 μm)).

The mineralogical counts, being approximations of the volume percentages of each grain type in the different sand size classes, were converted to weight percentages, using the approximate grain densities listed in Table 2. The densities chosen for lithic and mineral components were based on Deer et al. (1992), while the density of foraminifera is discussed by Miller and Komar (1977) and Oehmig (1993). Other biogenic components, being mainly built from CaCO_3 (which has a density of 2,700 kg/m^3) or SiO_2 , were given an estimated density of 2,000 kg/m^3 . The results were then applied to the grain size frequency distributions of the sands, in order to create separate frequency distributions for the grain types of interest (in this case being the quartz and feldspar grains and the foraminifera). Descriptive parameters, such as the median (or ' d_{50} ') could then be calculated for each grain type population within the sand fraction. They are listed in Table 3. Clearly, the d_{50} 's of the foraminifera fractions are higher than those of the quartz fractions.

Current meter records

The measurements (current speed and direction, and water temperature) recorded by the four current meters deployed in 2000 resemble each other closely. The time series are presented in Fig. 6 and an exceedance plot for the current data is shown in Fig. 7. The currents clearly show a semi-diurnal tidal character, with a c.7 day signal superimposed. This cycle is also clearly expressed by negative pulses in the temperature data. It is clear that for most of the time (>60%) the current speeds are higher than 10 cm/s, while currents exceeding 25 cm/s only occur for about 0.7–1.6% of the time. The maximum current speed recorded was 35.1 cm/s at station 11,572, east of the mound. Notably, the measurements in the 'tail' area seem to indicate slightly lower currents than at the other three stations.

The frequency distributions of the current speeds and directions are presented in rose diagrams in Fig. 8. Again

Fig. 4 a Results of the grainsize analyses on the bulk samples (*core logs*) and on the bulk sand fractions, where >20% (*graphs*). The sample depths are indicated, as are those samples used for further mineralogical analysis. **b** Example grainsize distribution of a sandy mud sample (lower part of boxcore 16/1), illustrating the uniform distribution of the fines

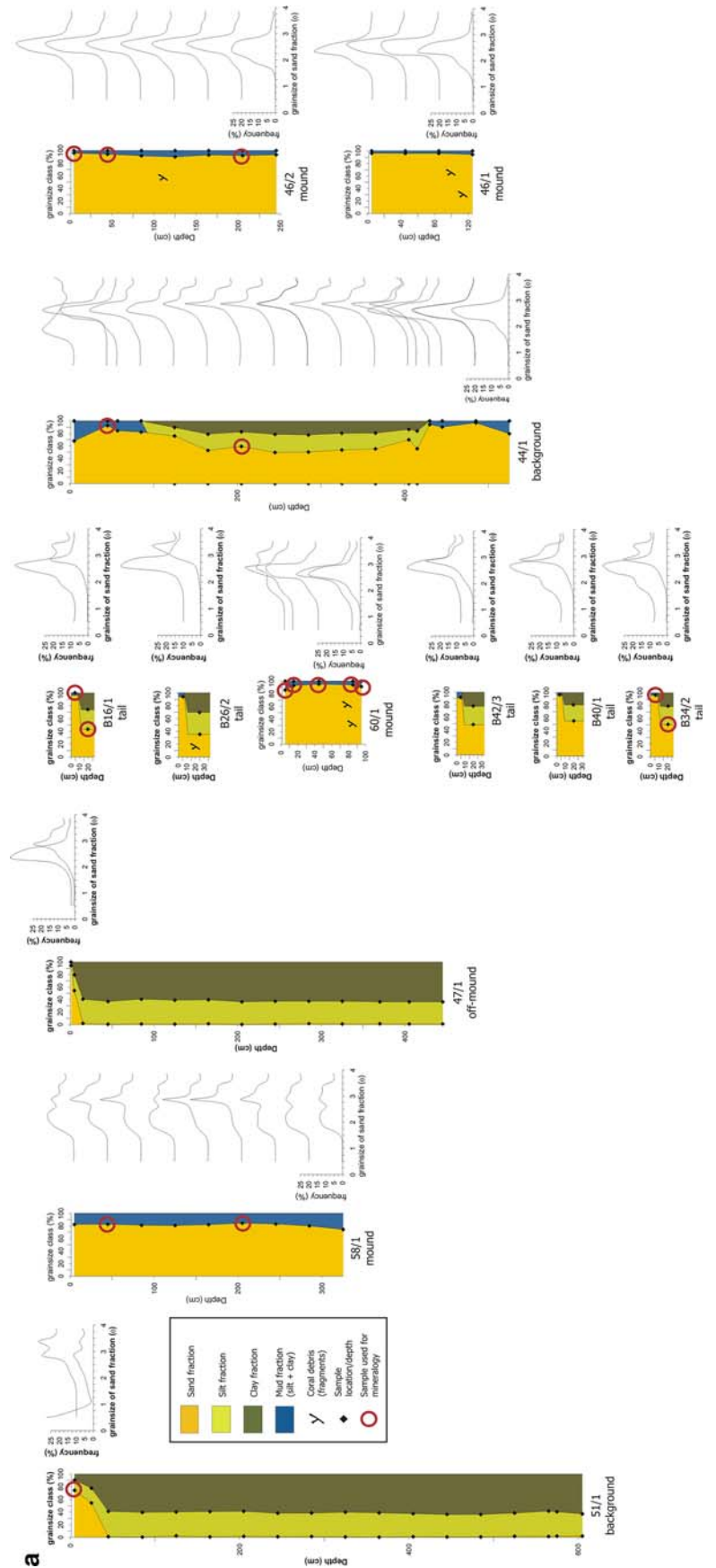
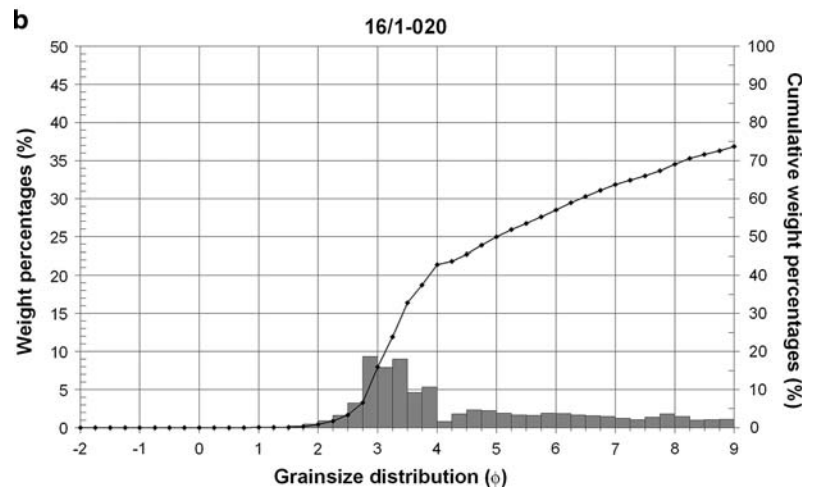


Fig. 4 continued



there are strong similarities between the four stations. The current direction with highest frequency lies between 225 and 247°N, indicating that the dominant tidal regime is aligned NE–SW. However, the strongest currents measured (>30 cm/s, occurring 0.2% of the time) had a more westward direction. The actual impact of these variations is revealed by the trajectory plots in Fig. 9. Apparently at the beginning of the measurement period there were 6–8 tidal cycles during which the ebb and flood directions were not opposed, but at an angle of nearly 90° to each other. This resulted in an overall southward residual current. The next 2 or 3 cycles consisted of the strong current event, possibly a so-called ‘benthic storm’, as defined by Hollister and McCave (1984), with an overall westward direction. After these two events the tidal signal became more regular, with SW–NE excursions, and maximum speeds reaching between 14 and 20 cm/s.

The overall residual currents (for the period from day 1 to 19: 13/07, 3:25–31/07, 4:20) are in the order of 1–1.4 cm/s, and directed ca. 195°N. However, as pointed out above, this result is strongly influenced by the first 4–5 days of the recordings. If only the last two weeks are taken into account (16/07, 09:25–31/07, 04:20), the residual current reduces to ca. 0.4 cm/s, and is directed between 200 and 255°N, in the direction of the main tidal component as illustrated by Fig. 8. Hence, it appears that, although the overall system is tidal, different regimes can act in the area, including the effects of short-lived events such as ‘benthic storms’. However, the deployment period of the current meters was too short to identify each of the different regimes clearly. Apart from that, there may also be seasonal variations, not recorded during this short-term experiment.

Sediment dynamics

Based on the results discussed above, some estimations are made of the critical shear stress and related current speed at

1 m above bottom, necessary for the erosion of the quartz/feldspar and the foraminifera sand fractions of the 17 samples analysed for mineralogical composition. A Shields-type criterion (Shields 1936; Miller et al. 1977) was used, expressed in the following formula from Soulsby (1997), developed for the transport of sands:

$$\frac{\tau_{cr}}{g(\rho_s - \rho)d} = \frac{0.30}{1 + 1.2D_*} + 0.055[1 - \exp(-0.020D_*)] \tag{1}$$

with: τ_{cr} threshold bed shear stress (N/m²), g acceleration due to gravity (9.81 m/s²), ρ_s grain density (kg/m³), ρ water density (at 8°C and 35.1 ppt: 1,027.4 kg/m³), d grain diameter, D_* dimensionless grain size

$$D_* = \left[\frac{g(\rho_s - \rho)}{\rho\nu^2} \right]^{1/3} d \tag{2}$$

with: ν : kinematic viscosity of water (at 8°C and 35.1 ppt : 1.4313 × 10⁻⁶ m²/s)

The critical shear stress τ_{cr} can be translated in a ‘critical shear velocity’ u_{*cr} :

$$u_{*cr} = \sqrt{\frac{\tau_{cr}}{\rho}} \tag{3}$$

Assuming a logarithmic current velocity profile in the water column (as approximation for transitional and turbulent flow), the critical current velocity for erosion at 100 cm above the bed ($u_{100,erosion}$) can be calculated as (Soulsby 1997):

$$u_{100,erosion} = \frac{u_{*cr}}{0.41} \ln \left(\frac{z_{100}}{z_0} \right) \tag{4}$$

with: z_{100} level above seabed, i.e. 1 m or 100 cm, z_0 roughness length

Due to the non-dimensionalisation (using the kinematic viscosity and the density of both the fluid and grains), the Shields criterion expressed in Eq. (1) can be used for all

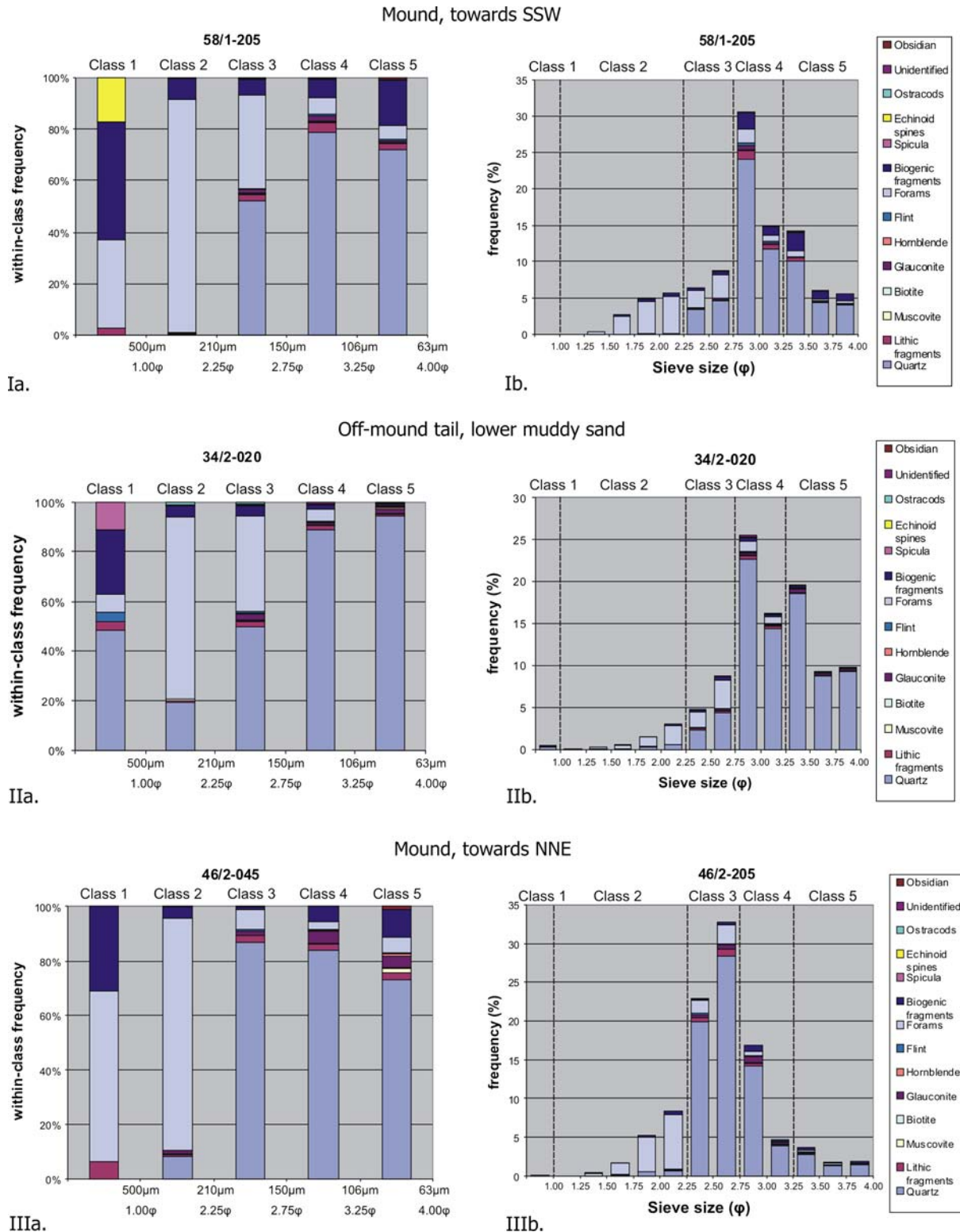


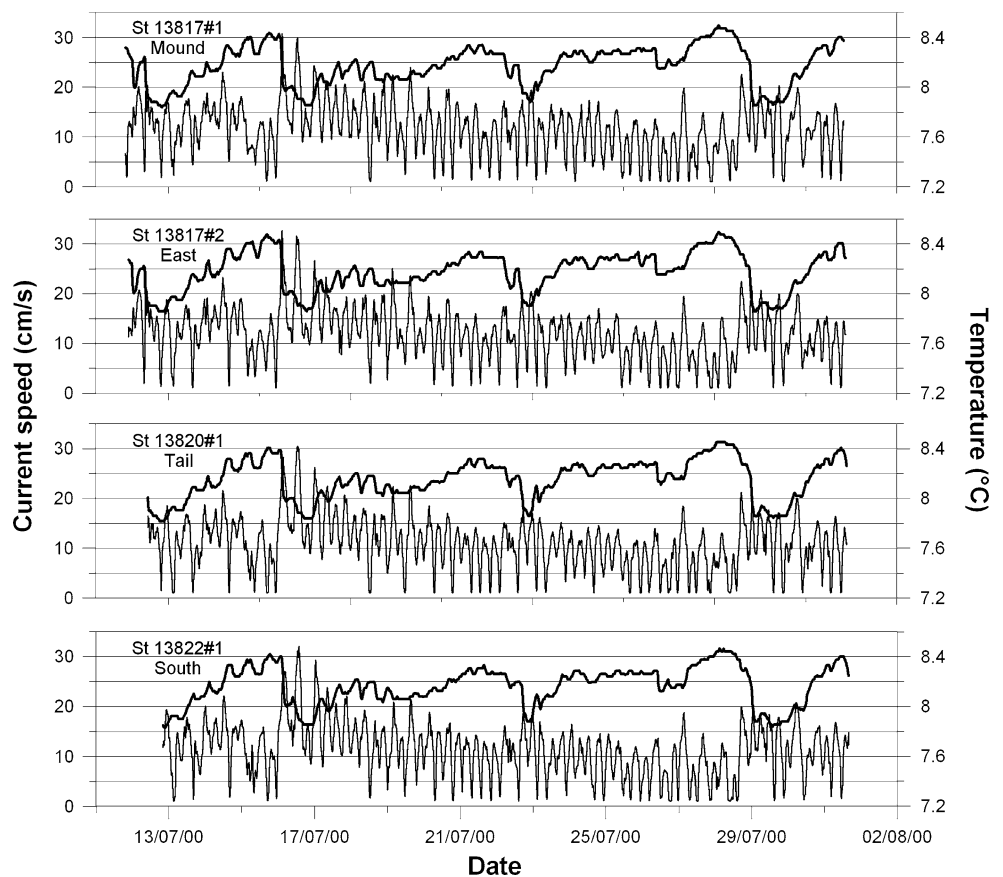
Fig. 5 Mineralogical composition of the sand fraction in three representative samples: **(a)** the five sand classes (see Table 2) and **(b)** representative of the whole grainsize spectra I **a & b**. Mound sample,

located towards the SSW, fine to very fine sands, II **a & b**. Off-mound ‘tail’ sample, lower muddy fine to very fine sand, III **a & b**. Mound sample, located towards the NNE, fine sand

Table 3 Critical erosion and deposition current velocities calculated for the quartz/feldspar and foraminifera fractions of the 17 samples analysed for mineralogy

Sample	d_{50} quartz (μm)	d_{50} forams (μm)	Quartz/feldspar			Foraminifera		
			$u_{100,erosion}$ (cm/s)	w_s (cm/s)	$u_{100,sett}$ (cm/s)	$u_{100,erosion}$ (cm/s)	w_s (cm/s)	$u_{100,sett}$ (cm/s)
46/2-005	164	229	35.14	1.37	37.43	22.34	0.79	20.91
46/2-045	164	230	35.14	1.37	37.43	22.35	0.80	21.07
46/2-205	161	237	35.10	1.33	36.26	22.38	0.84	22.20
44/1-045	154	215	35.01	1.22	33.57	22.26	0.70	18.72
44/1-205	126	195	34.56	0.84	23.49	22.12	0.58	15.72
34/2-005	165	242	35.15	1.39	37.82	22.41	0.87	23.01
34/2-020	112	192	34.27	0.67	18.94	22.10	0.57	15.29
60/1-005	105	208	34.10	0.59	16.81	22.21	0.66	17.65
60/1-015	132	218	34.67	0.92	25.56	22.28	0.72	19.18
60/1-045	144	235	34.86	1.08	29.84	22.37	0.83	21.87
60/1-085	154	238	35.01	1.22	33.57	22.39	0.85	22.36
60/1-095	151	236	34.97	1.18	32.44	22.38	0.83	22.04
16/1-005	164	244	35.14	1.37	37.43	22.42	0.89	23.34
16/1-020	104	180	34.08	0.58	16.51	22.01	0.50	13.60
58/1-045	123	221	34.50	0.80	22.48	22.29	0.74	19.65
58/1-205	126	232	34.56	0.84	23.49	22.36	0.81	21.39
51/1-005	100	180	33.97	0.54	15.35	22.01	0.50	13.60

Fig. 6 Current meter (fine) and temperature records (heavy line) for the 4 current meters indicated on Fig. 2. The semi-diurnal and c. 7 day tidal influences can clearly be recognised



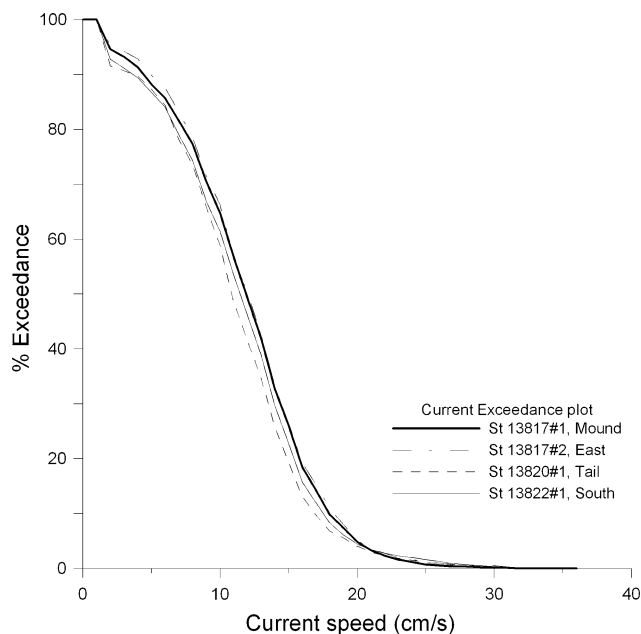


Fig. 7 Percentage current speed exceedance graph for the 4 current meters under study

circumstances in terms of sediment type, water conditions or even fluid characteristics. Alternatively, the nomograms in Miller et al. (1977), for quartz grains and in Miller and Komar (1977), for foraminifera sands, could be used, albeit after adaptation for the correct densities and seawater viscosity. It has to be noted that the formulae and graphs mentioned above strictly speaking apply to the erosion of a single grainsize fraction from a plane bed. Ripples or other bedforms may cause increased shear stresses, and mixed sediment types may cause larger grains to protrude into the water column and be picked up more easily. However, even if ripples have been recognised on the video fragments from the study area (Masson et al. 2003), they only form during high-current speed events, and are severely degraded in a few days by the biological activity of mainly seafloor dwelling organisms (Masson et al. 2004). Furthermore, the critical shear stress for the erosion of grains corresponds to the so-called ‘skin friction shear stress’ close to the bed, which in practice is calculated as the shear stress in case no bedforms were present (Soulsby 1997). Under these conditions the roughness length z_0 is equal to $d_{50}/12$. Concerning the sediment mixtures, the fact that large grains protrude and small grains are sheltered, suggests that the d_{50} actually may be a representative parameter to describe the sediment dynamics of the mixture. This is confirmed by Kleinhans (2004) who states that unimodal sediment mixtures tend to show near equal mobility of large and small grains, while in strictly bimodal mixtures the two modes more or less move according to the thresholds of each of the separate modes. In the

calculations described above, the d_{50} values were estimated for the quartz/feldspar & foraminifera populations of the sand fractions only, even if in the muddy sands and sandy muds a significant proportion of the sediment was actually found in the finer fractions. However, these fines are generally fairly uniformly distributed in a long ‘tail’, without a clear mode. Hence it is assumed that those d_{50} ’s, as an approximation of the centre and main mode of the sand fractions, are a better parameter to describe the hydrodynamic properties of the sediments under study than the d_{50} of the entire grainsize population.

In addition to the critical erosion velocity, deposition was also considered. When grains are eroded from the seabed, they first start moving as bedload (rolling, sliding, saltating). However, if the current speeds increase, or if the grains are smaller, they may become carried by the water flow as suspended material. This mode of entrainment can result in transport over longer distances, which often can continue at current speeds well below the erosional threshold. The deposition of a grain will then largely depend on its settling velocity in the water column, compared to the shear stress. Soulsby (1997) suggests that grains settle from suspension when the settling velocity w_s is equal to the skin friction shear velocity u_* :

$$w_s = u_{*,\text{setl}}$$

With w_s calculated as:

$$w_s = \frac{v}{d} [(10.36^2 + 1.049D_*^3)^{1/2} - 10.36] \quad (5)$$

Hence, for each of the d_{50} values, the critical current speed at 1 m above the bed could be calculated for which the grains would settle from suspension, using Eqs. 3, 4 and 5.

The results are presented in Table 3. It is clear that the critical velocity for erosion decreases from the N–NE to the S–SW of the study area, following the grainsize gradient. Given the natural (short-term) variability of bottom current speeds, a decrease from 35.14 to 33.97 cm/s appears rather minimal. However, estimating the maximal error on the d_{50} calculations as $\pm 5\%$ (i.e. 6.6 μm for the quartz grains, based on sensitivity analysis including errors on the sieving, grain counts and estimated densities), which results in a maximal variation in calculated critical current velocity in the order of ± 0.15 cm/s, the decrease is significant. It illustrates a typical characteristic of the physical process of erosion, namely that for the range of grainsizes under consideration here, very subtle changes in current velocity can have important consequences in terms of erosion and winnowing. At the actual seabed, this subtle decrease in estimated erosional threshold may translate in a gradual decrease in maximal current speed and/or frequency of occurrence of those current speeds up to 35 cm/s. A similar effect is seen for the foraminifera, although for lower

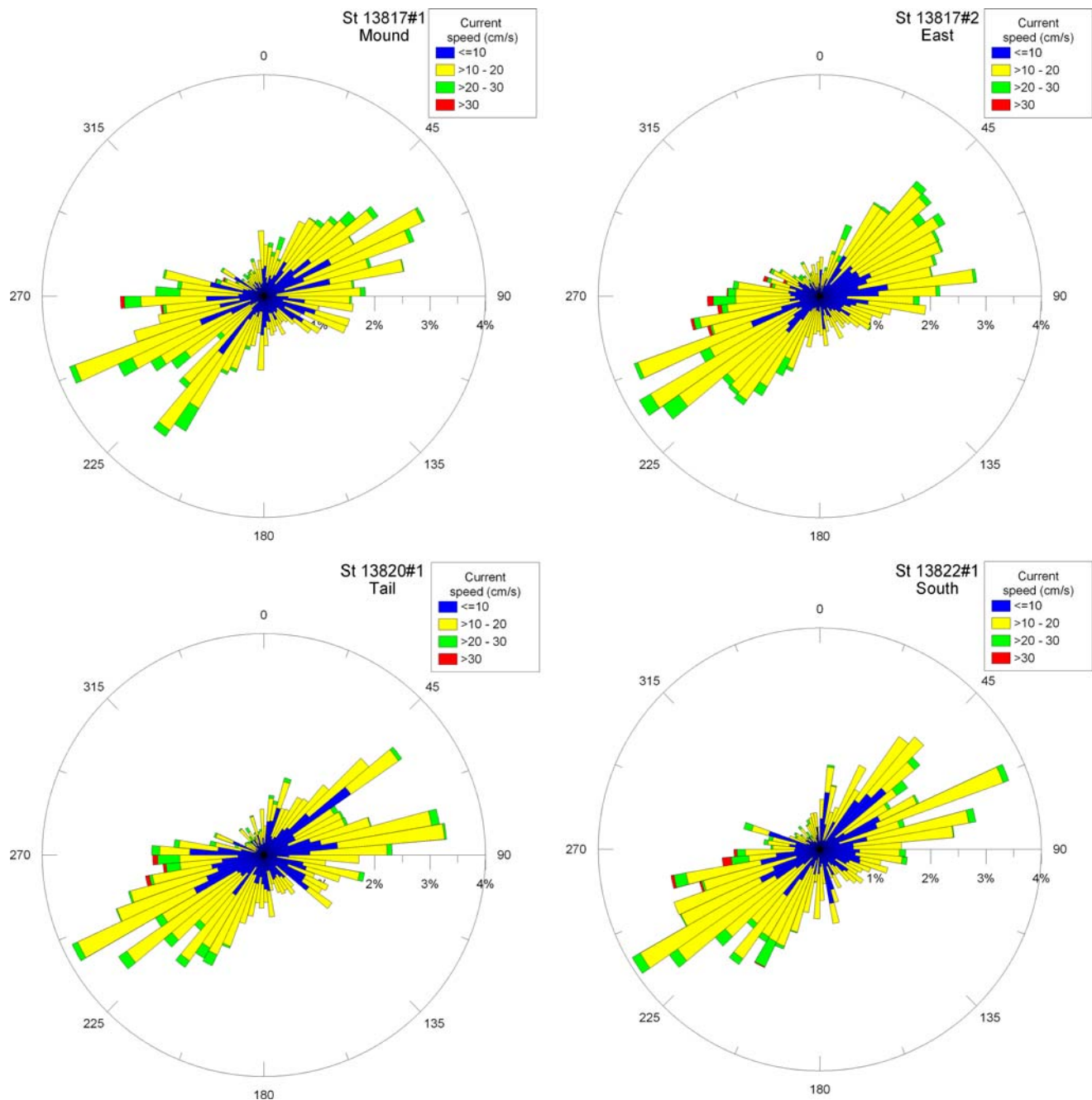
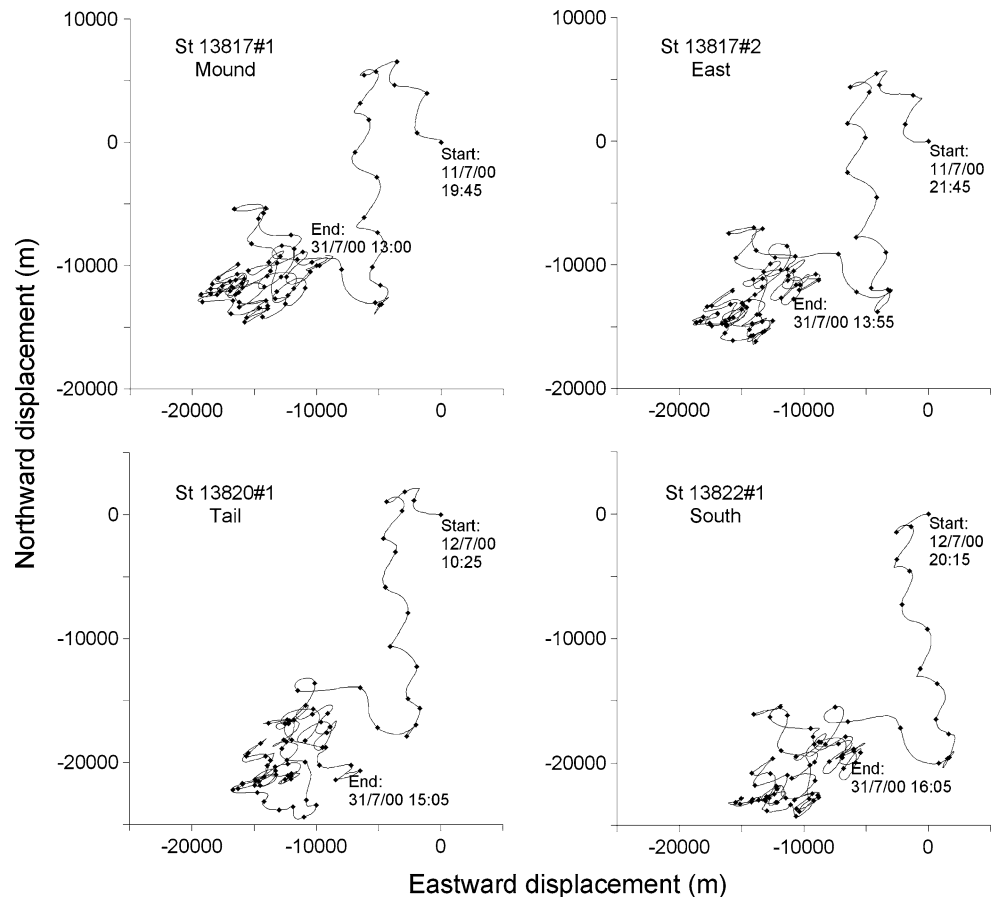


Fig. 8 Rose diagrams for the 4 current meters studied, indicating the frequency of occurrence of each current direction and speed (indicated in colour)

absolute current speed values. Therefore, it seems that the foraminifera sand fraction, despite the larger d_{50} , may be eroded slightly more easily than the quartz grains, keeping in mind, however, that the formulae were derived for ideal conditions, and not for mixed sediments. Furthermore, considering the current measurements described in paragraph 4.3, current speeds in the order of 22 and 34 cm/s are only reached ca. 3, resp. 0.1% of the time, limiting the erosion to short intervals.

The settling velocities, on the other hand, show a much wider range of values. The coarsest grains clearly settle directly from a bedload transport regime, and will not be transported at current speeds below the erosional threshold. However, further to the S-SW and in the finer grained sands, as the d_{50} 's decrease, the $u_{100, \text{setl}}$ become increasingly smaller than the $u_{100, \text{erosion}}$, indicating a depositional environment governed by settling from suspension. The same pattern is observed for both quartz/feldspar grains

Fig. 9 Trajectory plots for each of the 4 current meters indicated on Fig. 2. Marks indicate 6-h intervals



and foraminifera. Although the foraminifera fraction is eroded at lower current speeds, it will also settle from bedload transport in the N–NE cores and coarser sands ($u_{100, \text{setl}}$ in the same order of magnitude as $u_{100, \text{erosion}}$). Further to the S–SW and in finer materials they also settle from suspension, at current speeds below ca. 14 cm/s, which is close to the lowest settling current speeds of the quartz grains (ca. 16 cm/s). The overall pattern illustrates how the study area is affected by current sorting.

Within the mound cores, as there seems to be a fining-upward trend (core 60/1 and visible within the foraminifera fraction of core 58/1; Fig. 4a), the deposition seems to have evolved from a bedload-dominated to a settling-from-suspension dominated system.

Discussion

The mineralogy and grain size distributions of the sands have shown that the mound sands have no exclusive characteristics. Overall, they follow the same regional trends as the off-mound seabed sands, which favours an interpretation of mound build-up through sediment baffling. Therefore, the interpretation of the surrounding sandy

contourite and its formation will be described first, leaving the discussion of the mound origin and formation mechanism to “[Corals and sand: Darwin mound formation](#)”. In addition, the fact that both the foraminifera and terrigenous (quartz/feldspar) fraction give separate but similar results, increases the confidence in the current-sorted interpretation described below.

Structure of the sandy contourite

Considering the upper sands in the off-mound cores (noting that the on-mound sands also concur), together with the background information on the hydrography of the area, the analysis results clearly confirm the interpretation of Masson et al. (2003) of a contourite sand sheet or a thin sandy contourite, as defined by a.o. Viana et al. (1998) and Stow et al. (2002a). Following the original definition of Heezen et al. (1966), they describe contourites as ‘sediments in relatively deep water, deposited or significantly reworked by stable geostrophic currents’. Several of the typical characteristics of a ‘mid-depth sandy contourite’ –which is, according to Viana et al. (1998), the ‘main type of true sandy contourite’— can be recognised in the Darwin mound area: a quite thin,

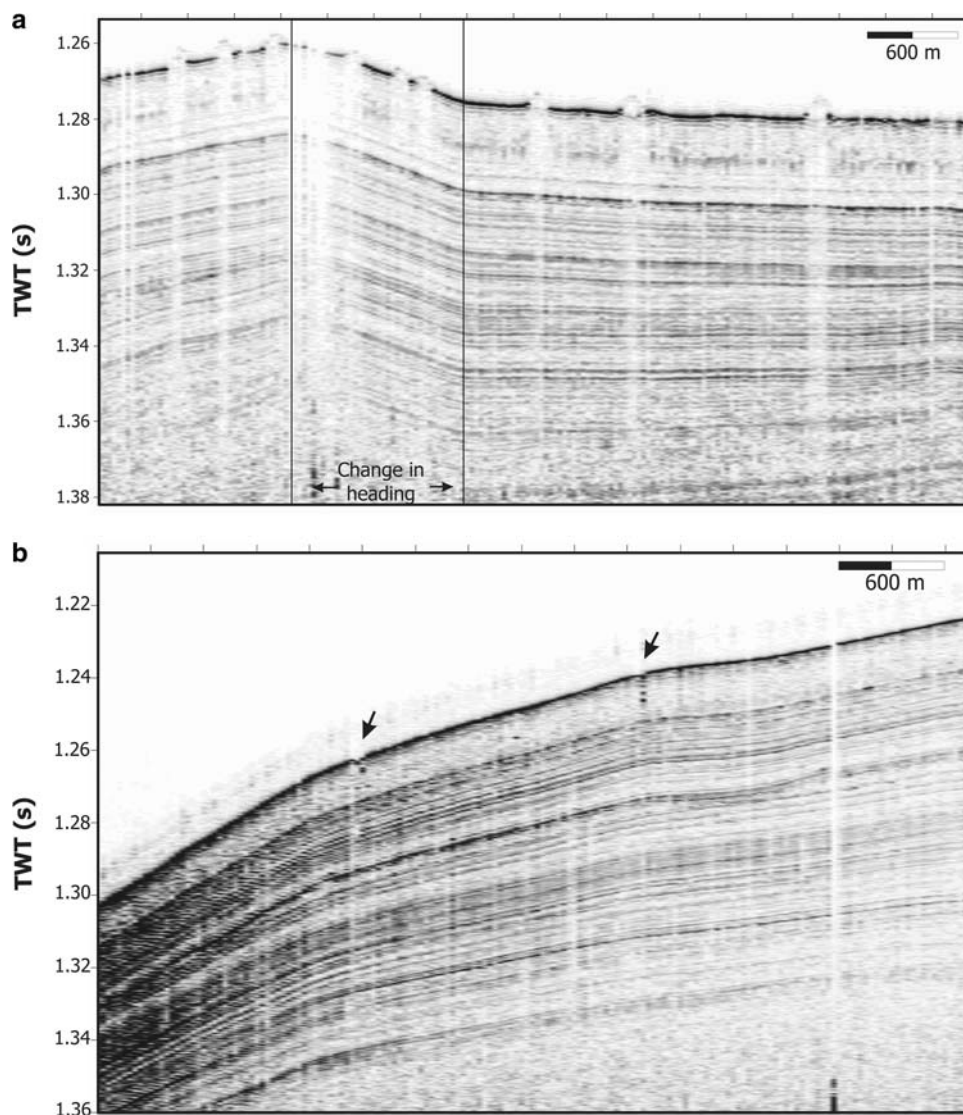
sheeted deposit, with a sharp or more gradational lower boundary, possibly containing ripples at the seabed and little or no primary structure remaining because of the high degree of bioturbation. The sands are mainly medium to fine, even grading into sandy silts, often relatively mud-free, and are moderately well sorted with a low to negative skewness. They have a mixed biogenic-siliciclastic composition and can be associated with muddy or silty contourites in lower sequences. Similar contourite sand sheets have been described for the wider area of the Rockall Trough and Faroe–Shetland Channel (e.g. on the Hebrides slope (Howe et al. 1994), the Barra Fan (Stow et al. 2002b), or the west-Shetland slope (Masson 2001; Plets 2003)). They are generally attributed to an along-slope geostrophic current, stronger on the shelf edge and upper slope and reducing in force towards greater depths (Stow et al. 2002b). McCave (1982) explains that this spatial variation in current strength is related to a variation in slope gradient, which indeed is often linked to the water depth (with the steepest gradients on the mid- to upper slopes of the continental margins).

Compared to most of the contourite studies, however, the data presented here describe the sandy contourite in more detail, also numerically. They allow us to refine the model of contourite formation and sediment sorting. The estimated critical current velocities illustrate that in the case of the Darwin mound area, the sand sheet is not simply an area of pure winnowing, as suggested by Stow et al. (2002b) for sandy contourites, but essentially is governed by depositional processes. Basically, at the seabed, a (sandy) contourite sheet represents an area where both ‘erosion’ and ‘deposition’ are acting constantly, or at least regularly. Along the current flow-path, every square meter can act as sediment source area for the adjacent square meter, but can also act as a deponent for the slightly coarser fraction eroded from the previous square meter. In most cases there will be a slight difference in the sediment input versus output which means either a net deposition or erosion (winnowing *sensu stricto*). McCave and Hall (2006) estimate that, with increasing current speeds, from a speed of about 10–15 cm/s indeed sediment sorting is no longer purely due to selective deposition, but is due to a combination of selective deposition and removal of fines (winnowing). Real erosional winnowing might occur above 20 cm/s, while they estimate that above 30 cm/s sands will be sufficiently mobile to form ripples and bedforms. These estimates are now confirmed by the sedimentological and numerical data presented here: towards the N–NE of the study area, the sands are governed by movement and settling under the form of bedload, under current speeds of minimum 25–35 cm/s that occur for only about 3% of the time. Towards the

S–SW, the effect of settling from suspension becomes the more and more important, both for foraminifera and quartz grains, indicating a gradual and subtle decrease in governing current speed to values in the order of 15 cm/s. The current variation occurs over a distance of 4.5–5 km only, and is clearly capable of sorting the fine sands and silts.

This spatial pattern also supports the model sketched by Viana et al. (2007), which indicates a bi-directional fining tendency typically observed in the sedimentary facies of sandy contourite systems. It is due to the current intensity reduction along the flowpath, and to a downslope effect related to the increasing distance from the current core. Zooming out to a wider area, this model can be nested in the regional hydrography as described under “[Hydrography](#)”. When the CSC is deflected to the S–SW by the WTR and Ymir Ridge, it is forced to flow around the head of the Rockall Trough and around the large sediment drift. The strongest part of the current, occurring on the shallowest and steepest parts of the WTR, causes winnowing and erosion, leaving a seabed with variable sedimentary composition, including a large amount of gravel. This is recognised on the regional TOBI sidescan sonar imagery as a high-backscatter area (Masson et al. 2003). As the bathymetric slope decreases along its path, e.g. from 2° to <1° in the area under study (based on the overall GEBCO bathymetry, GEBCO 2003), the current reduces in strength. Additionally, there is periodical across-contour (downslope) transport, such as illustrated for example by the 6–8 tidal cycles with overall S–SE net transport recorded by the current meters. The effect is that the high-backscatter area, on the large scale, consisting basically of winnowed and reworked glaciomarine sediments, acts as sediment source for the sandy contourite sheet. Within the contourite, the sediment then will be sorted further, still within a bi-directional spatial pattern. This is not a continuous process, but rather happens in ‘bursts’ when, due to a high current velocity event, the erosional threshold is exceeded. The result is visible on the TOBI sidescan (upper left corner of Fig. 2, or Masson et al. (2003)): the zone of lowest backscatter is an elongated area parallel to the contours, representing bedload deposition. The boundary with the upslope gravels is remarkably sharp, illustrating the efficiency of the sorting gradient (and the sensitivity of the sidescan system). Further downslope and along the current path, the backscatter grades into a slightly higher strength, where the d_{50} decreases and (slightly) more cohesive sediments are deposited (e.g. at the location of 51/1 and 58/1, and further to the S and SW). A similar interpretation of current decrease over the area is described by Wheeler et al. (2008) from bedform morphologies and backscatter strengths identified on high-resolution sidescan sonar data.

Fig. 10 TOPAS high-resolution profiles across (a) several Darwin mounds (profile indicated on Fig. 2) and (b) two of the pockmarks located to the SW of the mounds



Corals and sand: Darwin mound formation

Now that the sedimentary environment is described, the question of mound origin and formation can be addressed. The data presented above do not support the idea that the pistoncores taken on the mounds contain sands deposited under a process of fluid expulsion, as suggested by Masson et al. (2003). Several arguments can be listed. Firstly, as stated above, the sands in the mounds have comparable characteristics to the sands on the surrounding seabed. It is possible that the sand source for the sand volcanism was a contourite sheet similar to the one on the present-day seabed. However, the upward fining trend in core 60/1 does not support the idea of deposition under a sudden fluid expulsion event. The same is true for the presence of coral fragments within the sands, although they are limited in abundance, and probably could have been worked into the sediments by other mechanisms (e.g. burrowing or the

occurrence of small gravity flows on the flanks of the suggested sand volcanoes). It may be that the fluid expulsion was an episodic process, hence creating fining upward sequences and burying coral fragments. However, the trends in core 60/1 are very gradual, with no sharp boundaries, which does not support a depositional process based on episodic 'events'.

Apart from the sedimentological evidence, the TOPAS profile through some of the Darwin mounds (Fig. 10a) does not show any obvious pipe structures or disruptions below the mounds, which could indicate strong fluid escape from depth. There is partial amplitude reduction under the mounds, but this could be attributed to scattering of the acoustic signal, which is very focussed (typical for the TOPAS technology, Webb (1993)) on the mound surfaces and coral framework. From ca. 15 ms TWT below the mounds, all reflections are continuous. Cores containing more than 8 m of glaciomarine mud have been recovered

from the area (Masson et al. 2003), hence a possible sandy contourite, acting as sand source, should be located deeper than 8 m, but most probably shallower than the continuous reflections below 15 ms TWT (ca. 13.5 m depth). For completeness, it has to be pointed out that the west-ward continuation of the TOPAS profile, crossing the pockmark area, only shows clear disruption below a few pockmarks, while in most cases there are no indications for pipes or fluid flow structures (Fig. 10b). If such signature does occur, it seems to reach to a depth of ca. 10 ms TWT, to the same continuous reflector that may be the only possible candidate for a past sandy contourite under the mounds.

Strictly speaking, also, none of the mound cores studied here penetrated an entire mound and reached its base. Hence the deposits representing the actual mound initiation are probably not registered. Based on the similarity in spatial positioning pattern between the Darwin mounds and pockmarks, it is possible that some type of fluid expulsion activity was the trigger for mound formation. However, it is clear that the later build-up of the mounds was caused by sediment baffling, within the dynamics of the developing contourite sand sheet. A similar conclusion was drawn by Wheeler et al. (2008) based on the change in mound morphology over the Darwin mound province: mounds towards the N–NE are more elongated and modified by the currents, while those closer to the crest of the sediment drift are more circular, possibly inheriting their shape from a fluid expulsion event.

Based on principles described in the literature, a possible model for the actual baffling process can be described as follows: on the small scale, a single coral colony will form a permeable obstacle of limited size (ca. 25 cm high). An approaching current will be slowed down, but depending on the permeability, the form drag created by the body will be smaller than for a solid ‘bluff body’ of the same size (Allen 1982). The result is that the formation of a horseshoe vortex and the associated crescent scour, characteristic for obstacle marks, are disturbed and often cannot take place. Also the typical return eddies, formed at the so-called ‘re-attachment point’ behind the obstacle, will not develop when the porosity of the body is more than ca. 30% (Castro 1971). However, the turbulence intensity of the flow that enters the wake will be reduced compared to the oncoming flow (Allen 1982). Overall, this results in the reduction of the erosive power of the current in the immediate vicinity of the coral, and in the deposition of the coarsest fractions carried by that current (especially bedload). Sediments carried higher up in the water column, will stay suspended, as the turbulence above the coral may be increased because of the form drag. Allen (1982) also mentions that the degree of permeability of the object has a negative correlation with the reduction of the current speed, as the flow passes through the obstacle, but it has a positive correlation with

the distance behind the body over which the effect can be measured. Once the porosity reaches values $>30\%$, the effect is recordable until a distance of ca. 30 times the obstacle height, which would correspond to ca. 7.5 m behind a coral colony. Hence, on a mound, where the corals are spaced in the order of meters apart (Masson et al. 2003), the current speed is more or less continuously reduced, although in large parts this reduction might be no more than by 10 or 20% (Allen 1982). On the other hand, the description of the contourite sand sheet has shown that in this environment a subtle variation in current speed will result in net sediment deposition: the build-up of the Darwin mounds. To gain full insight in the actual process of sediment baffling by the cold-water corals, further numerical and physical modelling would be necessary.

The mounds themselves, once they start building up, form larger and more solid obstacles to the flow than the single corals, even if initially they are rather low and the coral cover only forms a ‘buffer’ against potential erosion of the upstream side (as would happen on sediment waves or dunes, for example (Kleinhans 2004)). In general, because the mounds, due to their formation history, are (or become, see Wheeler et al. 2008) fairly well streamlined, the amount of upstream scour on the seabed is also rather limited. But vortices may be formed around the structures and be shed downstream, which may cause the development of scour depressions and elongated sand shadows (Karcz 1968; Werner et al. 1980). The presence of a sand shadow can be inferred in a few cases from the high-resolution sidescan sonar data presented by Wheeler et al. (2008), while the ‘tails’ observed on the TOBI data may represent areas of limited deposition or ‘scour’.

The last question to be answered is why *Lophelia pertusa* prefers the contourite sand sheet, and why the mounds are formed there. Several observations in shallower water depths on the flanks of the WTR have shown plenty of hard settling grounds for the corals, present under a strong current regime. Based on the general environmental requirements for *Lophelia*, as described in the introduction, these could be possible places for coral occurrence and mound formation. However, coral occurrence seemed to be remarkably low (Bett 2001; Masson et al. 2003). Most probably the current regime is too fierce, and the corals may have difficulties to cope with it. Similar observations have been reported from certain areas in the Porcupine Seabight and Porcupine Bank, where large coral banks are presently void of life coral, most probably because of too strong currents (Foubert et al. 2005; Wheeler et al. 2005a). It appears that the regimes on the lower slope are more attractive. The mobile sands do not form a major problem for the corals, indeed, small coral mounds have been reported from sandy seabeds in several occasions (e.g. Moira mounds, Wheeler et al. 2005c; Galicia Bank,

Lavaley and Duineveld 2003). When current speeds reduce even further, and sediments become even finer, it probably becomes more difficult for the polyps to keep the sediments from ingestion, and the advection of food particles may be too low. The fact that small mounds can be formed in the Darwin area, is due to the fact that there is sufficient sediment input available for the structures to build up. If there would not be any sediment input, the corals would probably still be able to create a reef, in the style of the Sula Ridge, for example (Freiwald et al. 2002), but that would be fully based on a coral framework build-up, which in a later stage may be filled with sediment. The Darwin mounds on the other hand are largely built of sediment, with a much lower coral content.

Conclusions

Detailed grainsize and mineralogical analysis of piston- and boxcores, together with current meter results from the Northern Rockall Trough gave insight in the well-sorted sandy contourite that forms the sedimentary environment of the Darwin cold-water coral mounds. The contourite sheet, formed under recent (Holocene) hydrodynamic conditions, is governed by subtle depositional processes. It shows a clear bi-directional gradient in grain sizes, both in the terrigenous and the foraminifera fractions, which can be related to current velocity gradients, caused by a reduction in slope angle along the flow and by the increasing distance from the core of the flow in a downslope direction.

Furthermore, the results also show that the Darwin mounds, although they may have initiated through a process related to pore water expulsion, are built up through the baffling of current-sorted sandy sediments, derived from the contourite sand sheet forming around them. Acting as permeable obstacles, the cold-water corals slow down the periodical bottom current sufficiently for it to deposit part of its sediment load.

Acknowledgments The authors would like to thank the captain, crew and scientific party of the RRS Discovery cruise 248, during which the main dataset was gathered. The British Antarctic Survey (BAS), in the person of C. Pudsey and P. Morris, is thanked for the provision of and help with the TOPAS data. The cores were sampled and stored in the BOSCORF National Marine Facility. We would like to thank Tj. van Weering and B. Pratt for their helpful reviews. We also gratefully acknowledge the support from the EC FP5 RTN EURODOM (EC contract no HPRN-CT-2002-00212), from the FWO-Flanders (Belgium), and from the EC FP6 IP HERMES (EC contract no GOCE-CT-2005-511234, funded by the European Commission's Sixth Framework Programme under the priority 'Sustainable Development, Global Change and Ecosystems') during the course of this research. At the moment of submission, V. Huvenne was holder of a EC FP6 Marie Curie Intra-European Fellowship (project SEDCORAL, EC contract no MEIF-CT-2004-009412) and had a honorary post-doctoral mandate of the FWO-Flanders (Belgium).

References

- Allen JRL (1982) Sedimentary structures, their character and physical basis. vol 2. Developments in sedimentology, 30B. Elsevier, Amsterdam, pp 663
- Belderson RH, Kenyon NH, Wilson JB (1973) Iceberg plough marks in the northeast Atlantic. *Paleogeogr Palaeoclimatol Palaeoecol* 13:215–224
- Bett BJ (2001) UK Atlantic margin environmental survey: introduction and overview of bathyal benthic ecology. *Cont Shelf Res* 21: 917–956
- Bett BJ, Billet DSM, Masson DG, Tyler PA (2001) RRS discovery cruise 248—a multidisciplinary study of the environment and ecology of deep-water coral ecosystems and associated seabed facies and features (The Darwin Mounds, Porcupine Bank and Porcupine Seabight) Southampton Oceanography Centre, Cruise report 36, pp 52
- Burrows M, Thorpe SA (1999) Drifter observations of the Hebrides slope current and nearby circulation patterns. *Ann Geophysicae* 17:280–302
- Castro IP (1971) Wake characteristics of two-dimensional perforated plates normal to an air-stream. *J Fluid Dyn* 46:599–609
- Cohen JK, Stockwell JW Jr (2002) CWP/SU: seismic Un*x release no 39: a free package for seismic research and processing. Centre for wave phenomena, Colorado School of Mines
- De Mol B, Van Rensbergen P, Pillen S, Van Herreweghe K, Van Rooij D, McDonnell A, Huvenne V, Ivanov M, Swennen R, Henriët JP (2002) Large deep-water coral banks in the Porcupine Basin, southwest of Ireland. *Mar Geol* 188:193–231
- Deer WA, Howie RA, Zussman J (1992) An introduction to the rock-forming minerals, 2nd edn. Prentice-Hall, Harlow, pp 549
- Ellet DJ (1998) Norwegian sea deep water overflow across the Wyville–Thomson Ridge during 1987–88. *ICES Coop Res Rep* 225:195–205
- Ellet DJ, Roberts DG (1973) The overflow of norwegian sea deep water across the Wyville–Thomson Ridge. *Deep Sea Res* 20:819–835
- Ellet DJ, Edwards A., Bowers R (1986) The hydrography of the Rockall Channel—an overview. *Proc R Soc Edinb* 88B:61–81
- Foubert A, Beck T, Wheeler AJ, Operderbecke J, Grehan A, Klages M, Thiede J, Henriët JP, The Polarstern ARK-XIX/3a Shipboard Party (2005) New view of the Belgica mounds, Porcupine seabight, NE Atlantic: preliminary results from the Polarstern ARK-XIX/3a ROV cruise. In: Freiwald A Roberts JM (eds) Cold-water corals and ecosystems. Springer-Verlag, Heidelberg, pp 403–415
- Freiwald A (2002) Reef-forming cold-water corals. In: Wefer G et al (eds) Ocean margin systems. Springer-Verlag, Heidelberg, pp 365–384
- Freiwald A, Roberts JM (2005) Cold-water corals and ecosystems. Springer-Verlag, Heidelberg, pp 1243
- Freiwald A, Hühnerbach V, Lindberg B, Wilson JB, Campbell J (2002) The sula reef complex, norwegian shelf. *Facies* 47:179–200
- GEBCO (2003) GEBCO digital atlas: centenary edition of the IHO/IOC general bathymetric chart of the oceans. British Oceanographic Data Centre, Liverpool, 2 CD-ROM
- Hansen B, Østerhus S (2000) North Atlantic–Nordic seas exchanges. *Prog Oceanogr* 45:109–208
- Heezen BC, Hollister CD, Ruddiman WF (1966) Shaping the continental rise by deep geostrophic contour currents. *Science* 152:502–508
- Henriët JP, De Mol B, Pillen S, Vanneste M, Van Rooij D, Versteeg W, Croker PF, Shannon PM, Unnithan V, Bouriak S, Chachkine P, the Porcupine-Belgica '97 Shipboard party (1998) Gas hydrate crystals may help build reefs. *Nature* 391:648–649

- Hollister CD, McCave IN (1984) Sedimentation under deep-sea storms. *Nature* 309:220–225
- Hovland M (1990) Do carbonate reefs form due to fluid seepage? *Terra Nova* 2:8–18
- Hovland M, Judd AG (1988) Seabed pockmarks and seepages, impact on geology, biology and the environment. Graham & Trotman Ltd., London, pp 293
- Hovland M, Talbot MR, Qvale H, Olausen S, Aasberg L (1987) Methane-related carbonate cements in pockmarks of the north sea. *J Sediment Petrol* 57(5):881–892
- Howe JA, Humphery JD (1995) Photographic evidence for slope-current activity, hebrides slope, NE Atlantic ocean. *Scott J Geol* 30(2):107–115
- Howe JA, Stoker MS, Stow DAV (1994) Late cenozoic sediment drift complex, northeast Rockall Trough, north Atlantic. *Paleoceanography* 9(6):989–999
- Howe JA, Stoker MS, Stow DAV, Akhurst MC (2002) Sediment drifts and contourite sedimentation in the northeastern Rockall Trough and Faroe–Shetland Channel, North Atlantic Ocean. In: Stow DAV, Pudsey CJ, Howe JA, Faugères JC, Viana AR (eds) Deep-water contourite systems: modern drifts and ancient series, seismic and sedimentary characteristics. *Memoirs. Geological Society, London*, pp 65–72
- Huthnance JM (1986) The rockall slope current and shelf-edge processes. *Proc R Soc Edinb* 88B:83–101
- Huvenne VAI, Bailey WR, Shannon P, Naeth J, di Primio R, Henriot JP, Horsfield B, de Haas H, Wheeler A, Olu-Le Roy K (2007) The Magellan mound province in the Porcupine Basin. *Int J Earth Sci* 96:85–101
- Karcz I (1968) Fluvial obstacle marks from the wadis of the Negev (southern Israel). *J Sediment Petrol* 38(4):1000–1012
- Kenyon NH, Akhmetzhanov AM, Wheeler AJ, van Weering TCE, de Haas H, Ivanov M (2003) Giant carbonate mud mounds in the southern Rockall Trough. *Mar Geol* 195:5–30
- Kiriakoulakis K, Bett BJ, White M, Wolff GA (2004) Organic biogeochemistry of the Darwin mounds, a deep-water coral ecosystem, of the NE Atlantic. *Deep-Sea Res I* 51:1937–1954
- Kleinmans MG (2004) Sorting in grain flows at the lee side of dunes. *Earth Sci Rev* 65:75–102
- Knutz PC, Jones EJW, Howe JA, van Weering TCE, Stow DAV (2002) Wave-form sheeted contourite drift on the Barra Fan, NW UK continental margin. In: Stow DAV, Pudsey CJ, Howe JA, Faugères JC, Viana AR (eds) Deep-water contourite systems: modern drifts and ancient series, seismic and sedimentary characteristics. *Memoirs. Geological Society, London*, pp 85–97
- Laberg JS et al (2005) Cenozoic alongslope processes and sedimentation on the NW European Atlantic margin. *Mar Petrol Geol* 22:1069–1088
- Lavaley MSS, Duineveld GCA (2003) A long-term settlement experiment near *Lophelia* thickets at the Galicia Bank (NW Spain). In: Freiwald A, Roberts JM (eds) 2nd International symposium on Deep-Sea Corals. Institut für Geologie der Universität Erlangen-Nürnberg, Erlangen, Germany, pp 55
- LeBas T (2002) PRISM—processing of remotely-sensed imagery for seafloor mapping. Version 4. Southampton Oceanography Centre, Southampton, internal report pp 196
- Masson DG (2001) Sedimentary processes shaping the eastern slope of the Faeroe–Shetland Channel. *Cont Shelf Res* 21:825–857
- Masson DG, Jacobs CL (1998) RV colonel templar cruises 01 and 02/98. TOBI surveys of the continental slope north and west of Scotland. Southampton Oceanography Centre, cruise report 22, pp 50
- Masson DG, Howe JA, Stoker M (2002) Bottom-current sediment waves, sediment drifts and contourites in the northern Rockall Trough. *Mar Geol* 192:215–237
- Masson DG, Bett BJ, Billett DSM, Jacobs CL, Wheeler AJ, Wynn RB (2003) The origin of deep-water, coral-topped mounds in the northern Rockall Trough, Northeast Atlantic. *Mar Geol* 194:159–180
- Masson DG, Wynn RB, Bett BJ (2004) Sedimentary environment of the Faroe–Shetland and Faroe Bank Channels, north-east Atlantic, and use of bedforms as indicators of bottom current velocity in the deep ocean. *Sedimentology* 51(6):1207–1241
- McCave IN (1982) Erosion and deposition by currents on submarine slopes. *Bulletin de l'Institut de Géologie du Bassin d'Acquitaine* 31:47–55
- McCave IN, Hall IR (2006) Size sorting in marine muds: processes, pitfalls and prospects for paleoflow-speed proxies. *Geochem Geophys Geosyst* 7(10): Q10N05
- Michels KH (2000) Inferring maximum geostrophic current velocities in the Norwegian–Greenland Sea from settling-velocity measurements of sediment surface samples: methods, application and results. *J Sediment Res* 70(5):1036–1050
- Mienis F, de Stigter HC, White M, Duineveld G, de Haas H, van Weering TCE (2007) Hydrodynamic controls on cold-water coral growth and carbonate mound development at the SW and SE Rockall Trough margin, NE Atlantic ocean. *Deep Sea Res I* 54:1655–1674
- Mienis F, van Weering T, de Haas H, de Stigter H, Huvenne VAI, Wheeler AJ (2006) Carbonate mound development at the SW Rockall Trough margin based on high resolution TOBI and seismic recording. *Mar Geol* 233(1–4):1–19
- Miller MC, Komar PD (1977) The development of sediment threshold curves for unusual environments (Mars) and for inadequately studied materials (foram sands). *Sedimentology* 24:709–721
- Miller MC, McCave IN, Komar PD (1977) Threshold of sediment motion under unidirectional currents. *Sedimentology* 24:507–527
- New A, Smythe-Wright D (2001) Aspects of the circulation in the Rockall Trough. *Cont Shelf Res* 21:777–810
- Oehmig R (1993) Entrainment of planktonic foraminifera: effect of bulk density. *Sedimentology* 40:869–877
- Plets RMK (2003) Sedimentology of a thin holocene sand sheet deposited by bottom currents in the Faeroe–Shetland Channel. Msc thesis, University of Southampton, Southampton, pp 49
- Roberts DG, Bott MHP, Uruski C (1983) Structure and origin of the Wyville–Thomson Ridge. In: Bott MHP, Saxov S, Talwani M, Thiede J (eds) Structure and development of the Greenland–Scotland Ridge: new methods and concepts. *Nato conference series IV: marine sciences. Plenum Press, New York*, pp 133–158
- Roberts JM, Wheeler AJ, Freiwald A (2006) Reefs of the deep: the biology and geology of cold-water coral ecosystems. *Science* 312:543–547
- Shields A (1936) Application of similarity principles and turbulence research to bedload movement, vol 167. *Hydrodynamics Laboratory, California Institute of Technology, Pasadena*, pp 36
- Soulsby R (1997) Dynamics of marine sands. A manual for practical applications. Thomas Telford Publications, London, pp 249
- Stoker MS, Akhurst MC, Howe JA, Stow DAV (1998) Sediment drifts and contourites on the continental margin off northwest Britain. *Sediment Geol* 115:33–51
- Stoker MS, Hitchen K, Graham CC (1993) The geology of the Hebrides and West Shetland shelves, and adjacent deep-water areas. HMSO for the British Geological Survey, London, Official regional report 2, pp 149
- Stow DAV, Armishaw JE, Holmes R (2002a) Holocene contourite sand sheet on the Barra Fan slope, NW Hebridean margin. In: Stow DAV, Pudsey CJ, Howe JA, Faugères J-C, Viana AR (eds) Deep-water contourite systems: modern drifts and ancient series, seismic and sedimentary characteristics. *Geological Society,*

- London, memoirs. The Geological Society of London, London, pp 99–119
- Stow DAV, Faugères J-C, Howe JA, Pudsey CJ, Viana AR (2002b) Bottom currents, contourites and deep-sea sediment drifts: current state-of-the-art. In: Stow DAV, Pudsey CJ, Howe JA, Faugères J-C, Viana AR (eds) Deep-water contourite systems: modern drifts and ancient series, seismic and sedimentary characteristics. Memoirs. The Geological Society, London, pp 7–20
- Viana AR, Faugères J.-C., Stow DAV (1998) Bottom-current-controlled sand deposits—a review of modern shallow—to deep-water environments. *Sediment Geol* 115:53–80
- Viana AR, Almeida W Jr, Nunes MCV, Bulhões EM (2007) The economic importance of contourites. In: Viana AR, Rebesco M (eds) Economic and palaeoceanographic significance of contourite deposits. Special Publications. Geological Society, London, pp 1–23
- Webb DL (1993) Seabed and sub-seabed mapping using a parametric system. *Hydrographic J* 68:5–13
- Werner F, Unsöld G, Koopmann B, Stefanon A (1980) Field observations and flume experiments on the nature of comet marks. *Sediment Geol* 26:233–262
- Wheeler AJ, Beck T, Thiede J, Klages M, Grehan A, Monteys X, the Polarstern ARK XIX/3a Shipboard Party (2005a) Deep-water coral mounds on the Porcupine Bank, Irish margin: preliminary results from Polarstern ARK-XIX/3a ROV cruise In: Freiwald A, Roberts JM (eds) Cold-water corals and ecosystems. Springer-Verlag, Heidelberg, pp 393–402
- Wheeler AJ, Bett BJ, Billet DSM, Masson DG, Mayor D (2005b) The impact of demersal trawling on NE Atlantic deep-water coral habitats: the case of the Darwin mounds, UK. In: Barnes PW, Thomas JP (eds) Benthic habitats and the effects of fishing. America Fisheries Society, Bethesda
- Wheeler AJ, Kozachenko M, Beyer A, Foubert A, Huvenne VAI, Klages M, Masson DG, Olu-Le Roy K, Thiede J (2005c) Sedimentary processes and carbonate mounds in the Belgica mound province, Porcupine Seabight, NE Atlantic. In: Freiwald A, Roberts JM (eds) Cold-water corals and ecosystems. Springer-Verlag, Heidelberg, pp 571–603
- Wheeler AJ, Kozachenko M, Masson DG, Huvenne VAI (2008). The influence of benthic sediment transport on cold-water coral bank morphology and growth: the example of the Darwin Mounds, NE Atlantic. *Sedimentology* in press